ORIGINAL ARTICLE

Nr 2024;14 (4):553-566

Curcumin (*Curcuma longa*) Supplementation Associated with Low-Dose Prednisone Improves Morphofunctional, Histomorphometric and Postsynaptic Aspects of the Rectus Femoris Muscle in Old Female Wistar Rats with Experimental Rheumatoid Arthritis

Ana Caroline Barbosa Retameiro[1], Carolina de Toni Boaro[1], Diego Francis Saraiva Rodriguez[1], Taciane Stein[1], Aldair Casagrande dos Santos[1], Jurandyr Pimentel Neto[2], Adriano Polican Ciena[2], Márcia Miranda Torrejais[1], Rose Meire Costa[1], Gladson Ricardo Flor Bertolini[1], Lucinéia de Fátima Chasko Ribeiro[1]

[1] *Center of Biological and Health Sciences, State University of Western Parana, Cascavel, Parana, Brazil*
[2] *Laboratory of Morphology and Physical Activity (LAMAF), São Paulo State University, Rio Claro, São Paulo, Brazil*

CORRESPONDING AUTHOR:
Ana Caroline Barbosa Retameiro
Center of Biological and Health Sciences
State University of Western Parana
Universitária Street 2069
85819-110 Cascavel, Paraná, Brazil
E-mail: ana.retameiro@unioeste.br; anaretameiro@gmail.com

DOI:
10.32098/mltj.05.2024.05

LEVEL OF EVIDENCE: 3

SUMMARY

Objective. Rheumatoid arthritis (RA) is an inflammatory disease. Here we analyzed the effects of the supplementation with curcumin (CM) in a treatment with prednisone (PD) on hind paw' functionality and rectus femoris histomorphometric and immunohistochemical aspects.

Methods. Thirty female 18 months-old Wistar rats were divided in six groups: control (CG), arthritis (AG), arthritis CM (AC), arthritis PD low-dose (APLD), arthritis PD high-dose (APHD) and arthritis PD low-dose and CM (APLDC). The experimental RA was induced by a complete Freund's adjuvant injection into the knee joint cavity. PD (2 mg/kg/day and 10 mg/kg/day) and CM ($C_{21}H_{20}O_6$) (100 mg/kg/day) were used as treatment, using gavage method. Functionality, histomorphometric and immunohistochemical evaluations were performed in the hind paw and in the rectus femoris muscle. Generalized mixed models was used for statistical analysis. Statistical significance was set as P-value 0.05.

Results. AG had loss of grip strength, motor function and increase in nociceptive threshold ($p < 0.0001$). AC and APLDC had positive effects on grip strength and motor function. Histomorphometry revealed degenerative lesions in AG muscular tissue with circulatory disorders, changes in muscle fibers, connective tissue and muscle spindle, major total collagen quantity and smaller perimeter in the postsynaptic region ($p < 0.0001$). APLDC showed the best recovery in these aspects ($p < 0.001$).

Conclusions. CM supplementation in the treatment with 2 mg/kg/day of PD restored muscle strength, motor function, histomorphometrical and postsynaptic aspects in old female rats with experimentally induced RA.

KEY WORDS

Neuromuscular junction; turmeric; arthritis; morphometry; immunohistochemistry.

INTRODUCTION

Rheumatoid arthritis (RA) is a systemic autoimmune inflammatory disease, more frequently diagnosed in elderly females (1) around the age of 40 to 50 years (2) that results, predominantly, in synovial inflammation in multiple joints, causing pain, reduced mobility and overall comfort of life (3).

During RA progression, persistent inflammation leads to systematic changes and functional disability (3) causing periarticular manifestations such as muscle atrophy, and loss of mobility (1). The loss of muscle mass can affect the entire body, and, in this sense, muscle tissue analysis may be an important aspect in the evaluation of RA progression and treatment success (4).

Previous studies found that age and sex may influence the choice of treatment in RA. Elderly patients are more likely to receive glucocorticoids (5). Prednisone (PD) is one of most prescribed, which can inhibit secretion of pro-inflammatory cytokines (6). However, it shows low bioavailability because of its nonspecific distribution throughout the body, which increases the risk of adverse effects (7) such as infections, liver injury, gastrointestinal damage (8) and muscle weakness in patients with RA (9).

In this way, there is a need to address alternative treatments. Recent evidence recommends that active ingredients of herbal, used for medical purposes, have anti-inflammatory, immunomodulation, chondroprotective and anti-oxidation effects and can be used to improve the symptoms of RA (10). Curcumin (CM), a phenolic chemical active compound extracted from the rhizomes of turmeric (*Curcuma longa*), belongs to the ginger family, *Zingiberaceae*, and has various beneficial pharmacological and biological effects such as antioxidant, anti-inflammation, and anti-arthritic (11).

To sum up, it seems that CM has therapeutic potential for the treatment of RA, which may be mainly mediated by its immunomodulatory effects on a wide range of deficient immune cells (12). In this way, it has been suggested that CM could be used as a supplement-therapy associated with anti-rheumatic drugs (11). However, it has very low aqueous solubility, which leads to a decrease in its bioavailability (13) and regarding toxicological, safety and dosages, the data are still conflicting.

In this context, the aim of the current study was to analyze the effects of treatment with low dose of PD supplemented with CM on the hind paw functionality, histomorphormetric and immunohistological neuromuscular junctions' aspects in the rectus femoris muscle of 18 months old female Wistar rats with CFA-induced RA. It is hypothesized that supplementation can be able to potentiate the effects of the drug and attenuate its side effects.

METHODS

The study was approved by the Ethics Committee for Animal Use (CEUA nº 77-19/2020 – date of approval: February 14, 2020) of the State University of Western Parana (UNIOESTE) and was conducted according to the ethical guidelines of the International Association for the Study of Pain (14).

The animals were randomized into groups composed of Wistar female rats, aged 18 months and maintained at a controlled temperature of 21 ± 1 °C under a 12:12 hour light-dark cycle. For functional and histomorphometrical analysis, 30 rats were divided into the following groups (n = 5): Control Group (CG), Arthritis Group (AG), Arthritis Curcumin (AC), Arthritis Prednisone Low-Dose (APLD), Arthritis Prednisone High Dose (APHD) and Arthritis Prednisone Low-Dose and Curcumin (APLDC). For the immunohistochemical analysis 18 animals were grouped in similar fashion but with n = 3 for each group.

Protocols

Experimental arthritis induction

The experimental arthritis model was induced by a pre-sensitized intradermal injection of 50 µl CFA (0.5 mg/mL, *Mycobacterium butirycum*) into the tail base of animals in AG, AC, APLD, APHD and APLDC. However, CG received an injection of saline solution (sodium chloride 0.9%). Seven days after the first injection into the tail, an intra-articular injection of 50 µl (0.5 mg/mL, *Mycobacterium butirycum*) of CFA or saline solution was administered (**figure 1**). Furthermore, both injections were administered into the right tibiofemoral joint after tricomization and asepsis of the area with iodinated alcohol (1%) (15).

Supplementation with curcumin (Curcuma longa) in the treatment with prednisone

The treatment protocol for groups AC, APLD, APHD and APLDC started 24 hours after the intra-articular injection and was performed for 14 consecutive days by the gavage method (**figure 1**).

The animals were weighed before intra-articular injection and again, after one week of experiment to adjust the doses administered. GA received standard dose of water, AC; 100 mg/kg/day of dry extract of CM ($C_{21}H_{20}O_6$) (*Curcuma longa*) (16), APLD; 2 mg/kg/day (17) of PD, APHD; 10 mg/kg/day (18) of PD and APLDC; 100 mg/kg/day (16) of dry extract of CM ($C_{21}H_{20}O_6$) (*Curcuma longa*) + 2 mg/kg/day of PD.

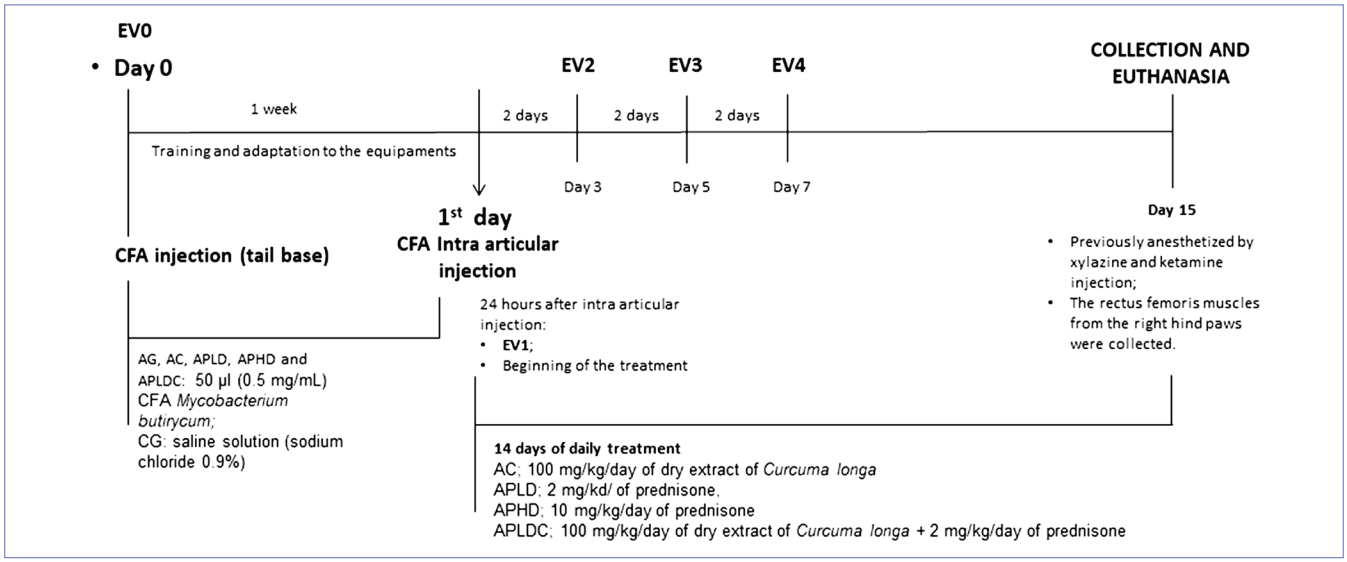


Figure 1. Schematic drawing demonstrating the chronological organization of the experiment.

Freund's Complete Adjuvant (CFA); Control Group (CG); Arthritis Group (AG); Arthritis Curcumin (AC); Arthritis Prednisone Low-Dose (APLD); Arthritis Prednisone High-Dose (APHD); Arthritis Prednisone Low-dose and Prednisone (APLDC); Evaluation 0 (EV0); Evaluation 1 (EV1); Evaluation 2 (EV2); Evaluation 3 (EV3) and Evaluation 4 (EV4).

Functional tests

The animals were submitted to simulated manipulation, for adaptation of the stimulus in all functional evaluation equipment, for 3 days. Then, they were submitted to 4 evaluation moments. Evaluation 0 (EV0) was performed on the day of the first sensitization at the base of the tail. Evaluation 1 (EV1), one day after the intra-articular injection, and Evaluations 2 (EV2), 3 (EV3) and 4 (EV4) occurred alternately every two days (**figure 1**). The results obtained in all EVs were recorded as an average between 3 consecutive trials (19).

Grip strength

The pelvic limb's grip strength was evaluated using a grip strength meter (Insight, Ribeirão Preto, São Paulo, Brazil) in all animals, as described by (20).

The animals were positioned such that it grasped a grid connected to a force transducer with its right hind paw and was then pulled by the tail with increasing force until the grip was eventually lost. The device provided the force in grams (g) exerted by the animal, and it was recorded as the average of three consecutive trials. The left hind paw was immobilized by the evaluator's hand to avoid interference.

Inclined plane

Motor function was evaluated using an inclined plane (Insight, Ribeirão Preto, São Paulo, Brazil). The test measured the animal's ability to stay on the top of a ramp whose inclination increased by 5° every 5 seconds. The inclined-plane test score was defined by the maximum angle reached by each animal while remaining on the ramp without slipping for at least 5 seconds. Measurements were made with the animal positioned in the transverse plane (vertical position) (21).

Von Frey

To assess the nociceptive threshold, a Von Frey filament digital analgesimeter (Insight, Ribeirão Preto, São Paulo) was used. The animal was positioned in an elevated box with a mesh floor, allowing the positioning of the filament perpendicular to the plantar region of the hind paw, with increasing pressure until the animal withdraws the limb, which provides the mechanical allodynia (g) of rodents (22).

Collection and euthanasia

On the 15th day after the experimental arthritis induction, animals were anesthetized using intraperitoneal injection of xylazine and ketamine. The proximal portions of the rectus femoris muscle and fixed in methacarn for histomorphometric analysis. The distal portions of the rectus femoris muscle were cryopreserved in liquid nitrogen at -195.8 °C and then stored in an ultrafreezer at -80ºC for immunohistochemical analysis (**figure 1**).

Light microscopy

The rectus femoris muscles of the right paw were collected, subjected to routine laboratory tests, fixed in methacarn.

After, the samples were dehydrated in an upward alcohol series, diaphanized using xilol, and embedded in histological paraffin. Subsequently, a microtomy was performed by obtaining 7-µm transversal sections using an Olympus microtome (R CUT 4055 Tokyo, Japan). Then, the slides were stained with hematoxylin and eosin (HE), to evaluate the histomorphometric aspects of the muscles, and with picrosirius red, to assess the types of collagens. After, photomicrographed using a light microscope (Olympus DP71, Tokyo, Japan) and polarized light microscope (Zeiss Axio Scope A1, Zeiss Industrial Metrology, Germain).

Morphological evaluation of rectus femoris muscle

Morphological analysis was performed to evaluate the effect of inflammation on the muscular tissue and were made using patterns (**supplement 1**) based on the type of pathological tissue change according to the main pathologies described by DeGirolami *et al.* (23) and adapted by Zazula *et al.* (24). These kinds of alterations are possibly related to the inflammatory processes caused by RA injuries. The processes of interstitial edema and hyperemia are directly associated with the chains of the inflammation processes and are related to the morphological changes analyzed (25).

Two values were used for the quantitative assessment of histopathology:

1. Importance factor (w), which takes into account the pathological importance of the change: 1- minimal importance, 2- moderate importance, 3- great importance.
2. Score value (a), which varies according to the extent of the change: 0- none, 2- minimal, 4- moderate, and 6- wide occurrence.

After getting these values, a mathematical calculation for injury rates was made for the total evaluation of the tissue. The score value for each change (a) is multiplied by the importance factor (w), resulting in the change index ($x = a \times w$). The sum of all x reflects the extent of occurrence of that pattern in the tissue revealing the total damage index (25).

Histomorphometric evaluation of the rectus femoris muscle

For the general histomorphometric analysis, the proximal portion of the rectus femoris muscle was fixed in methacarn solution and stained in H/E and in picrosirius red. The cross sections stained in H/E were used for the quantification of nuclei, central nuclei, muscle fibers and capillaries in 10 fields per animal.

For each field, 10 fibers were selected to perform measurements of area (µm²), major and minor diameter (µm) and 10 nuclei were selected to quantify the nuclei area (µm²). Muscle spindles were also analyzed through capsule diameter (µm) and area (µm²). These measurements were performed using the Image-Pro Plus 6.0 program.

The cross sections stained in picrosirius red were used for the quantification, in pixels percentage (%), of total collagen and it's different types by color, where type I was red and type III, green, in 10 fields per animal, in relation to the total collagen present in each field. These measurements were performed using the GNU Image Manipulation Program (GIMP 2.10.34).

Immunohistochemistry

The samples of rectus femoris (n = 3 in each) of experimental groups were dissected and cryo-fixed in liquid nitrogen (-196ºC), and performed longitudinal sections (10 µm thickness) (Cryostat HM 505 E, MICROM™). Such sections were collected in salinized slides, pre-treated with 3% EDTA solution, and washed (3 × 5 min) in phosphate-buffered saline (PBS), permeabilized in Triton-X 0.1% (10 min) and blocked with PBS and 1% of bovine serum albumin (BSA) (20 min). After, the sections were incubated overnight at 4 °C in a solution containing α-bungarotoxin conjugated rhodamine (BTX; Molecular Probes™, Eugene, OR-T-1175), diluted 1:600 in PBS and 1% BSA. The rectus femoris muscle sections were then washed in PBS (3 × 5 min) before being coated with Prolong (Molecular Probes™, Eugene, OR- P10144).

Neuromuscular junction morphometry

For the neuromuscular junction analysis, 30 images were used for each experimental group taken by an Olympus BX61™ Fully Motorized Fluorescence Microscope (Shinjuku, Japan) equipped with a Fluorescence UIS2. The images were obtained using a monochromatic camera Orca-Flash 2.8 (Hamamatsu, Japan), with the CellSens 11 Software (Olympus™) in 1,000X magnification.

After, were measured with ImageJ™ software the neuromuscular junction variables: stained area (µm²), total area (µm²), stained perimeter (µm), total perimeter (µm), dispersion (%) regarding the variables of area relation, and the postsynaptic cleft maximum diameter (µm) to determine the higher distance between their limits.

Statistical analysis

The results are expressed as mean ± SD for all parameters tested. A mixed generalized model test with Fisher (LSD) post-hoc test was used for the functional evaluations (grip strength, inclined plane and Von Frey).

For the morphological and histomorphometric variables, a mixed generalized model test with Sidak post-hoc test was used. These tests were performed in the Statistical Package for the Social Sciences (SPSS) program.

For the NJM morphometry, data were analyzed using Kruskal-Wallis with Dunn's post-hoc test by GraphPad Prism™ 8.4.3.
Statistical significance was set at p = 0.05.

RESULTS

Body mass

Body mass measurement showed a difference between the first and second week with weight loss in all groups (p = 0.0004). AG was different from all groups, with the greatest loss (4.4% of initial weight), followed by APHD, with 2.7%, and APLD, with 2.5% loss, being the groups that came closest to of AG (APHD: p = 0.048, APLD: p = 0.031). AC and APLDC had 1.4% and 1.2% loss, respectively, and were statistically equal to CG (AC: p = 0.267, APLDC: p = 0.423), which had only 0.35% loss (**table I**).

Functional tests

Grip strength test

Grip strength showed no interaction between groups and EVs (p = 0.876). However, differences were observed between groups (p < 0.0001) (**figure 2.1 A**) and between EVs (p < 0.0005) (**figure 2.2 A-F**).
Among the groups, all differed in GC p (p < 0.0001). AG had the lowest muscle strength value, not statistically different from APLD (p = 0.139) and followed by APHD. AC and APLDC, on the other hand, obtained the closest values to CG (AC: p = 0.0001, APLC: p = 0.0002) (**figure 2.1 A**).
Between the evaluations, all groups with experimental arthritis (AG, AC, APLD, APHD and APLDC) had lower values in EV1, performed 24 hours after the intra-articular injection and in EV2, when compared to EV0 (EV1: p < 0.0002, EV2: p < 0.0005). And in EV4 the values were equal to EV0 (p = 0.827) (**figure 2.2 A-F**).

Inclined plane test

In the motor function evaluation performed through inclined plane test, there were differences between the groups (p = 0.008) (**figure 2.1 B-F**), evaluations (p < 0.0008) (**figure 2.2 G-L**), and there was interaction between groups and evaluations (p = 0.007). Between groups, in EV1 AC (p = 0.003), APLD (p = 0.002) and APHD (p = 0.009) values decreased when compared to CG. In EV2, AG (p = 0.015), APLD (p = 0.009) and APHD (p = 0.0001) were different from CG, while AC (p = 0.060) and APLDC (p = 0.089) already showed recovery in the values. In EV3, all the treated groups had the same values as CG (AC: p = 0.259, APLD: p = 0.187, APHD: p = 0.710, APLDC: p = 0,256). In EV4, APLD had a new drop in values, and differed from CG (p = 0.005), as well as AG (0.024) which remained with low values in all EVs. On the other hand, AC (p = 0.256), APHD (p = 0.850) and APLDC maintained values equal to CG (**figure 2.1 B-F**).
Within the groups throughout the EVs, AG, APLD and APLDC had a decrease in the values in EV1 (AG: p = 0.002, APLD: p < 0.0002, APLDC: p = 0.003) which remained until EV4 (AG: p = 0.005, APLD: p < 0.001, APLDC: p = 0.038). AC (p = 0.002) and APHD (p = 0.002) also had reduced values in EV1, but APDH returned to initial values in EV3 (p = 0.090), which remained until EV4 (p = 0.446) and AC in EV4 (p = 0.186). CG had equal values in all EVs (**figure 2.2 G-L**)

Von Frey test

Nociceptive threshold, performed through the Von Frey test, showed difference between groups (p < 0.0001) (**figure 2.1 G-K**), evaluations (p < 0.0008) (**figure 2.2 M-R**) and interaction between both (p < 0.0002).
Among the groups, all animals that underwent arthritis induction had a reduction in values in EV1 (p < 0.0001), which remained until the last EV. However, in EV4 all treat-

Table I. Body mass in grams (g) in the first and second week of experiment and the difference of weight (g) between the two periods.

	1st week	2nd week	Difference
CG	280.8 ± 15.6	279.8 ± 15.6	-1 ± 2^{A}
AG	288.67 ± 31.9	276 ± 31.7	-12.7 ± 2^{C}
AC	283.7 ± 22.5	279.7 ± 20.6	-4 ± 3^{AB}
APLD	274.5 ± 23.2	267.7 ± 26.3	-6.8 ± 5.9^{B}
APHD	273.8 ± 15.4	266.5 ± 13.3	-7.3 ± 8.8^{B}
APLDC	269.7 ± 18.2	266.5 ± 17.7	-3.2 ± 5.3^{AB}

CG: Control Group; AG: Arthritis Group; AC: Arthritis Curcumin; APLD: Arthritis Prednisone Low-Dose; APHD: Arthritis Prednisone High-Dose; APLDC: Arthritis Prednisone Low-Dose and Curcumin. Different letters represent different values. Values are expressed as mean ± SD. A mixed generalized model test with Fisher (LSD) post-test was used (p = 0.05).

ed groups had values greater than AG ($p < 0.0001$) and APHD had values equal to CG ($p = 0.061$) (**figure 2.1 G-K**). Within the groups throughout the EVS, it was possible to notice that AG and APLD had a decrease in the values in EV1 when compared to EV0 ($p < 0.0001$), which remained until EV4 (AG: $p < 0.0004$, APLD: $p = 0.0001$). This also happened with AC ($p < 0.0009$), APHD ($p < 0.0006$) and APLDC (< 0.0007) in EV1. However, in EV4 AC ($p = 0.384$), APHD ($p = 0.769$) and APLDC ($p = 0.892$) returned to their initial values (**figure 2.2 M-R**).

Morphological analysis

In qualitative morphological analysis, the characteristic morphology of the rectus femoris muscle in CG could be observed, with predominantly polygonal-shaped fibers, arranged in connective tissue fascicles and with peripheral nuclei and blood vessels and nervous tissue with characteristic appearance (**figure 3A,H**).

All the arthritis groups presented general changes in muscle and associated tissues, circulatory disorders, changes in muscle fibers and connective tissue. However, AG

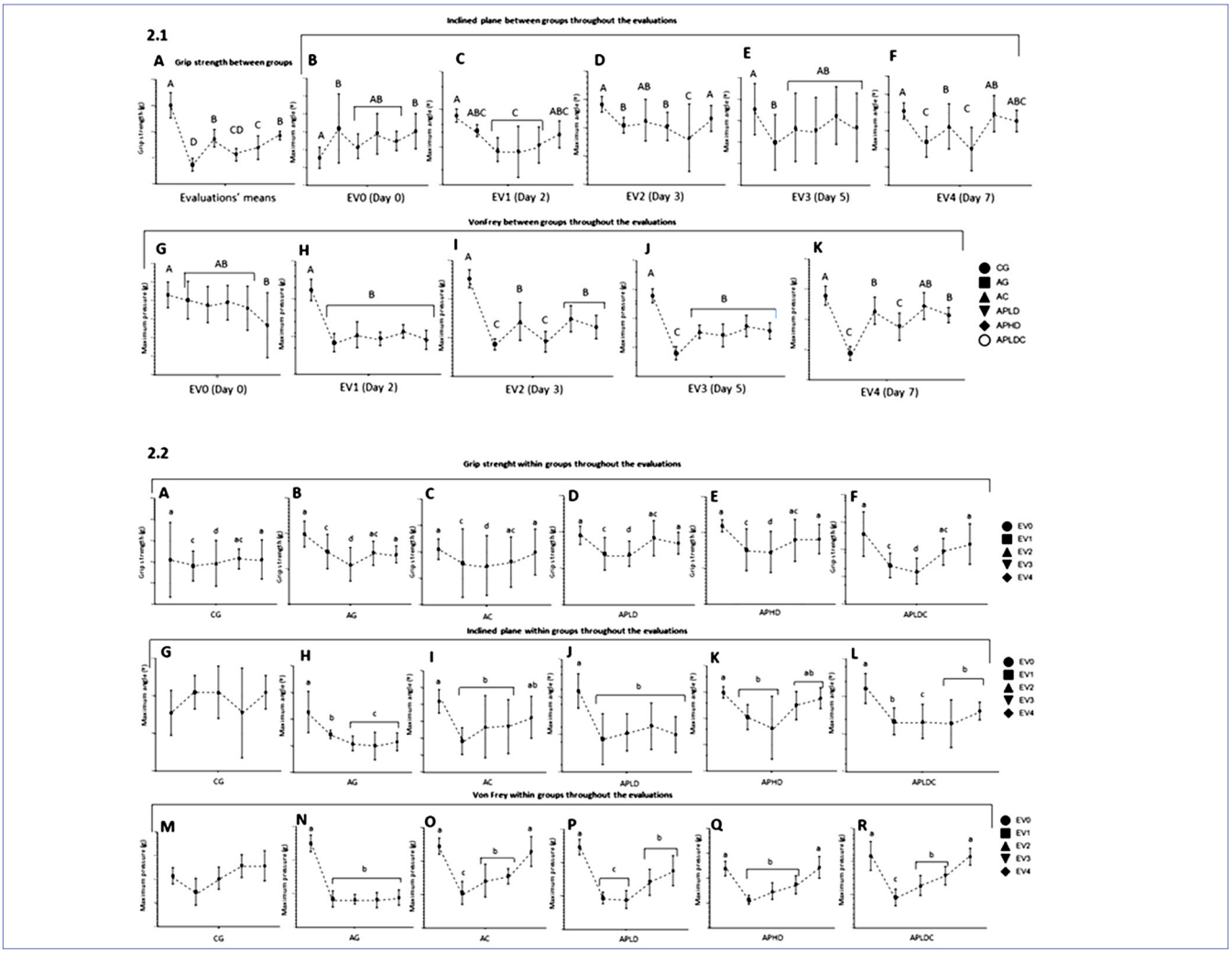


Figure 2. Functional tests results. Control Group (CG), Arthritis Group (AG), Arthritis Curcumin (AC), Arthritis Prednisone Low-Dose (APLD), Arthritis Prednisone High-Dose (APHD), Arthritis Prednisone Low-Dose and Curcumin (APLDC), Evaluation 0 (EV0), Evaluation 1 (EV1), Evaluation 2 (EV2), Evaluation 3 (EV3) and Evaluation 4 (EV4).

Different letters represent different values. Values are expressed as mean ± SD. A mixed generalized model test with Fisher (LSD) post-test was used ($p = 0.05$). 2.1: functional tests results between groups throughout the evaluations. **(A)** Grip strength (g); **(B-F)** Maximum angle reached by animals during the evaluations in the inclined plane (°); **(G-K)** Maximum pressure supported by the animals during the Von Frey test (g). 2.2: functional tests results within groups throughout evaluations. **(A-F)** Grip strength (g); **(G,L)** Maximum angle reached by animals during the evaluations in the inclined plane (°); **(M-R)** Maximum pressure supported by the animals during the Von Frey test (g).

presented severe and wide changes. In the muscle fibers it was possible to notice atrophic, rounded and degenerated fibers. The structures of nerves, spindles and connective tissue were affected by presence of adipose tissue and inflammatory processes. The blood vessels had an increase in blood flow which led to increased cell permeability due to the presence of inflammation. The nuclei were found in greater quantities, with basophilic halo and central nuclei were commonly found (**figure 3B,C,H**).

In the treated groups, although it was also possible to observe these alterations, they were milder and less extensive, mainly with a greater arrangement in the muscle fibers (**figure 3D-H**). However, APLDC was the group that seemed to have greater tissue organization and less alterations, being the one that most resembled CG (**figure 3G,H**).

In the quantitative assessment of histopathology, using the scores described in **table I**, it was possible to confirm the characteristics found in the morphological analysis with significant difference ($p < 0,0001$). When compared to CG, AG had the highest score ($p < 0,0001$) (**figure 3H**), followed by AC, APLD and APHD ($p < 0.0001$). APLDC had the lowest score among the treated groups, with a smaller difference in relation to CG ($p = 0.001$) (**figure 3H**).

Histomorphometric analysis of the muscle spindle

In the CG muscle spindle morphological analysis was possible to observe characteristic appearance with a bundle of specialized, striated, intrafusal fusiform spindle shaped muscle fibers, lying in parallel with the fascicles of the regular extrafusal muscle fibers and intact capsular structure (**figure 4A,G-H**). In AG it was possible to notice degeneration in all the morphological aspects, with complete disorganization in the intrafusal fibers and capsule (**figure 4B**).

In APHD, there was more organization when compared to AG, but it was still possible to observe disorganization in the intrafusal fibers (**figure 4E**). APLD presented the highest area and diameter values ($p = 0.001$) (**figure 4G-H**) of the capsule when compared to CG, however, together with AC and APLD, they were the groups that presented more characteristic morphological aspects and were closer to CG (**figure 4C-D,F**).

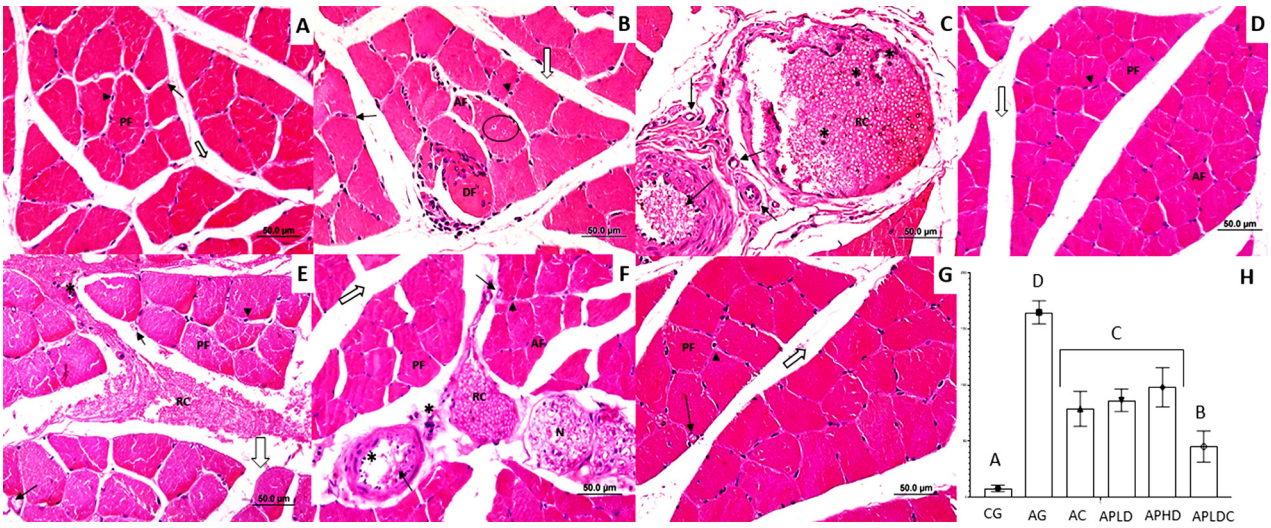


Figure 3. Photomicrographs of the Rectus Femoris muscle of female 18 months old Wistar rats in cross-section stained in HE.

(A) Control Group (CG), presenting standard aspects with polygonal fibers (PF), peripheral nuclei (black arrowhead), covered by connective tissue (white arrows), blood vessels and nerves entering in the muscle through bundles associated with connective tissue projections (black arrow); **(B,C)** Arthritis Group (AG) with marked changes showing degenerated fibers (DF), abnormal fibers (AF) central nuclei (black circle), changes in the arrangement of connective tissue (white arrow), hypertrophy in blood vessels (black arrow) with red cells (RC), and inflammatory cells (*); **(D)** Arthritis Curcumin (AC) group with polygonal fibers (PF), peripheral nuclei (black arrowhead), changes in the arrangement of connective tissue (white arrow); **(E)** Arthritis Prednisone Low-Dose (APLD) presenting Polygonal fibers (PF), peripheral nuclei (black arrowhead), connective tissue (white arrow), blood vessels (black arrow), red cells (RC) in the connective tissue and inflammatory cells (*); **(F)** Arthritis Prednisone High-Dose (APHD). Indicating polygonal fibers (PF), changes in the arrangement of connective tissue (white arrows), peripheral nuclei (black arrowhead), abnormal fibers (AF), blood vessels (black arrows) with red cells (RC), nerves (N) and inflammatory cells (*); **(G)** Arthritis Prednisone Low-Dose and Curcumin (APLDC) with polygonal fibers (PF), peripheral nuclei (black arrowhead), blood vessel (black arrow) and connective tissue (white arrow); **(H)** Averages of damage in the rectus femoris muscular tissue. Control Group (CG), Arthritis Group (AG), Arthritis Curcumin (AC), Arthritis Prednisone Low-Dose (APLD), Arthritis Prednisone High-Dose (APHD) and Arthritis Prednisone Low-Dose and Curcumin (APLDC). Different letters represent different values. Values are expressed as mean ± SD. A mixed generalized model test with Fisher (LSD) post-test was used ($p = 0.05$).

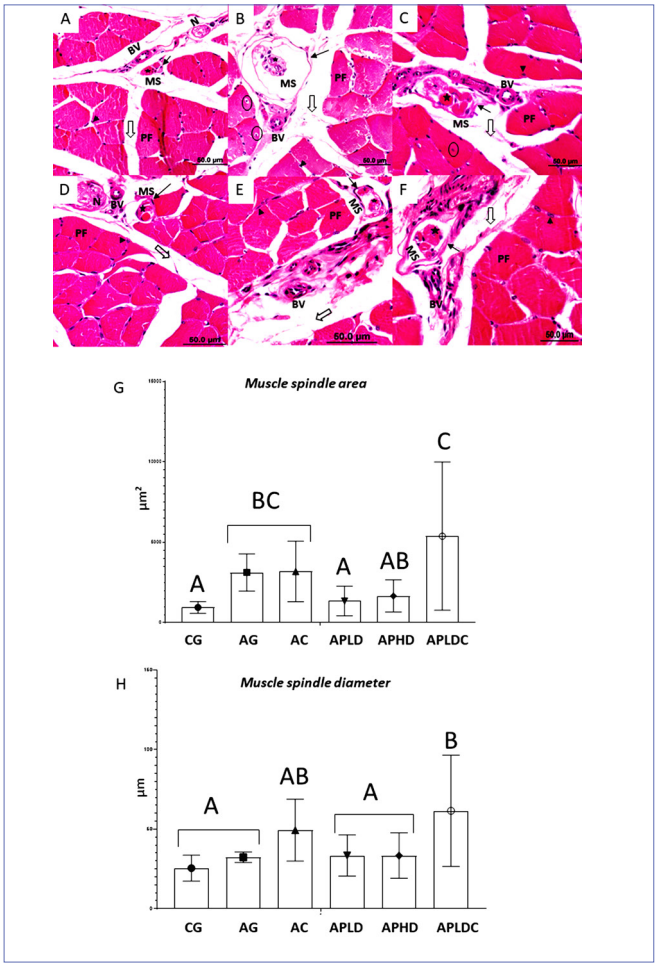


Figure 4. Photomicrographs of the Rectus Femoris muscle of female 18 months old Wistar rats in cross-section stained in HE. **(A)** Control Group (CG); **(B)** Arthritis Group (AG); **(C)** Arthritis Curcumin (AC); **(D)** Arthritis Prednisone Low-Dose (APLD); **(E)** Arthritis Prednisone High-Dose (APHD); **(F)** Arthritis Prednisone Low-Dose and Curcumin (APLDC). Are represented: polygonal fibers (PF), peripheral nuclei (black arrowhead), connective tissue (white arrows), muscle spindle (MS) with intrafusal fibers (star) and capsule (black arrow), central nuclei (black circle), nerves (N), blood vessels (BV). **(G,H)** Muscle spindle area **(G)** and Muscle spindle diameter **(H)**. Control Group (CG), Arthritis Group (AG), Arthritis Curcumin (AC), Arthritis Prednisone Low-Dose (APLD), Arthritis Prednisone High-Dose (APHD) and Arthritis Prednisone Low-Dose and Curcumin (APLDC). Different letters represent different values. Values are expressed as mean ± SD. A mixed generalized model test with Fisher (LSD) post-test was used (p = 0.05).

General morphometrical analysis

In morphometry, analysis of fiber area (**figure 5A**), major diameter (**figure 5B**) and total number of fibers (**figure 5E**), showed lower values in AG (p = 0.0013, p < 0.008, p = 0.0004), AC (p = 0.008, p = 0.0011, p = 0.028), APLD (p = 0.006, p = 0.002, p = 0.007) and APHD (p = 0.002, p = 0.0001, p = 0.005), when compared with GC. APLDC had values equal to GC (p = 0.971, p = 0.897, p = 0.903). In the minor fiber diameter (**figure 5C**), AG had the lowest value (p < 0.0007), followed by APHD (p < 0.0001), AC (p = 0.002) and APLD (p = 0.001). APLDC was equal to CG (0.840). Regarding the nuclei, in the total area (**figure 5D**), AG (p < 0.0002), AC (p < 0.0005) and APLD (p < 0.0003) had the highest values, followed by APHD (p = 0.003). APLDC was equal to APHD (P = 0.127) and CG (p = 0.131). In the total count (**figure 5F**) AG had the highest value (p < 0.0001), subsequently, APLD (p = 0.004) and AC was equal to AG (p = 0.087) and APLD (p = 0.706). APHD (p = 0.563) and APLDC (p = 0.976) had the same values as CG. In the count of central nuclei (**figure 5G**), AG had the highest value (p = 0.0002) and AC (p = 0.088), APLD (p = 0.234), APHD (p = 0.234) and APLDC (p = 0.844) were equal to CG.

In total capillary count (**figure 5H**) all groups were different from CG. APHD stood out with the highest result (p < 0.0005), followed by APLD (p = 0.0001), AG (p = 0.003), AC (p = 0.032) and APLDC (p = 0.001). The analyzes of nuclei/fiber ratio (**figure 5I**) and capillary/fiber ratio (**figure 5J**) showed no difference between groups.

Morphometrical analysis of collagen

In the quantification of total collagen, there was difference between groups (p < 0.0004). Compared to CG, AG had the highest value (p < 0.0004), followed by AC, APHD, APLD (p = 0.001) and APLDC (p = 0.003) (**figure 6A-G**). In the measurement of collagen type I (red) all arthritic groups had a higher amount when compared to CG. AG and APHD with p = 0.002, AC p = 0.005, APLD p = 0.001 and APLDC p = 0.003 (**figure 6A-F,H**).

Quantification of type III (green) showed no difference between groups (p = 0.648) (**figure 6I**).

Neuromuscular junction morphometry

The morphological aspects of the postsynaptic region were analyzed by immunostaining and the groups did not show great differences in this regard. All showed a compact and round morphology (**figure 7A-F**). Regarding morphometry, APLDC had greater total perimeter (CG p = 0.0025, AG p = 0.0097, AC p = 0.0003, APLD p = 0.0002, APHD p < 0.0001) (**figure 7H**). And in stained area (p = 0.0143) (**figure 7I**), stained perimeter (p = 0.0275) (**figure 7J**), minimum diameter (p = 0.0346) (**figure 7L**), g ratio (p = 0.0369) (**figure 7M**) and compactness (p = 0.0310) (**figure 7N**) APLDC differed only from APHD.

DISCUSSION

RA is the most common type of chronic joint inflammation and has high incidence in women that are passing through

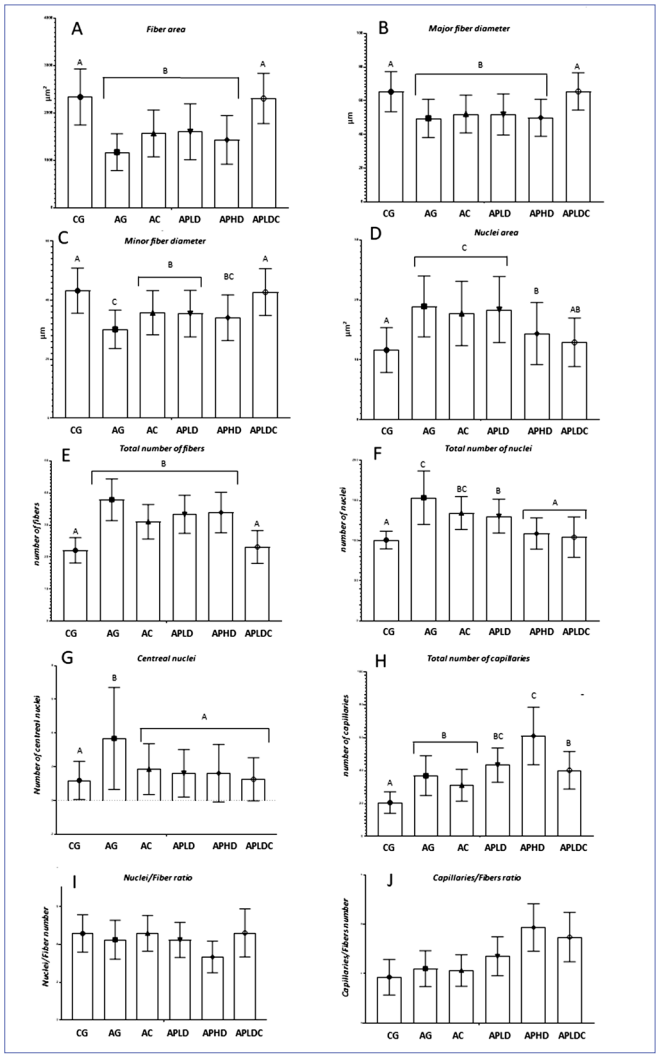


Figure 5. Morphometrical analysis of the rectus femoris muscle results.

Control Group (CG), Arthritis Group (AG), Arthritis Curcumin (AC), Arthritis Prednisone Low-Dose (APLD), Arthritis Prednisone High-Dose (APHD), Arthritis Prednisone Low-Dose and Curcumin (APLDC). Different letters represent different values. Values are expressed as mean ± SD. A mixed generalized model test with Fisher (LSD) post-test was used (p = 0.05). **(A)** Total fiber area; **(B)** Major fiber diameter; **(C)** Minor fiber diameter; **(D)** Nuclei area; **(E)** Total number of fibers; **(F)** Total number of nuclei; **(G)** Central nuclei account; **(H)** Total number of capillaries; **(I)** Nuclei/Fiber ratio; **(J)** Capillaries/Fibers ratio.

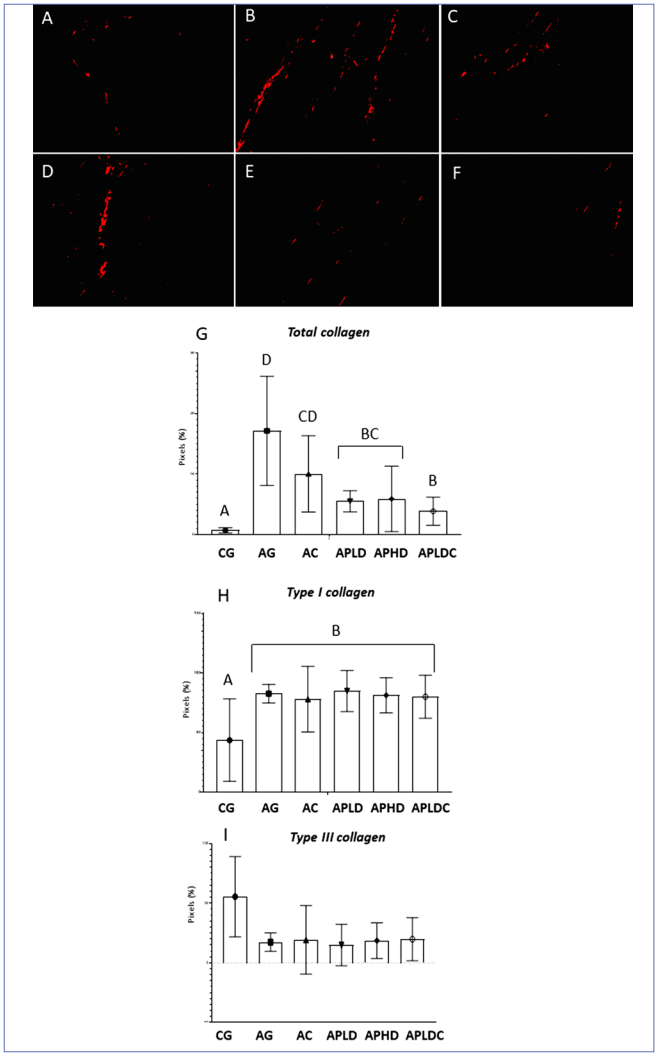


Figure 6. (A-F) Photomicrographs of the Rectus Femoris muscle of female 18 months old Wistar rats in cross-section stained in picrosirius red.

(A) Control Group (CG); **(B)** Arthritis Group (AG); **(C)** Arthritis Curcumin (AC); **(D)** Arthritis Prednisone Low-Dose (APLD); **(E)** Arthritis Prednisone High-Dose (APHD); **(F)** Arthritis Prednisone Low-Dose and Curcumin (APLDC); **(G-I)** Morphometrical analysis of the rectus femoris muscle results. Control Group (CG), Arthritis Group (AG), Arthritis Curcumin (AC), Arthritis Prednisone Low-Dose (APLD), Arthritis Prednisone High-Dose (APHD), Arthritis Prednisone Low-Dose and Curcumin (APLDC). Different letters represent different values. Values are expressed as mean ± SD. A mixed generalized model test with Fisher (LSD) post-test was used (p = 0.05); **(G)** Total quantification of collagen; **(H)** Quantification of Type I collagen; **(I)** Quantification of Type III collagen.

aging process. Our study showed that 14 days of supplementation with 100 mg/kg/day of CM dry extract, in the treatment with 2 mg/kg/day of PD, had significant benefits when compared to APHD, AG, APLD and APHD. We demonstrated the following main results.

AG had significant loss of body mass and APLDC had the best recovery

Chronic inflammatory diseases decrease body weight and induce muscle wasting. Muscle wasting is a common and

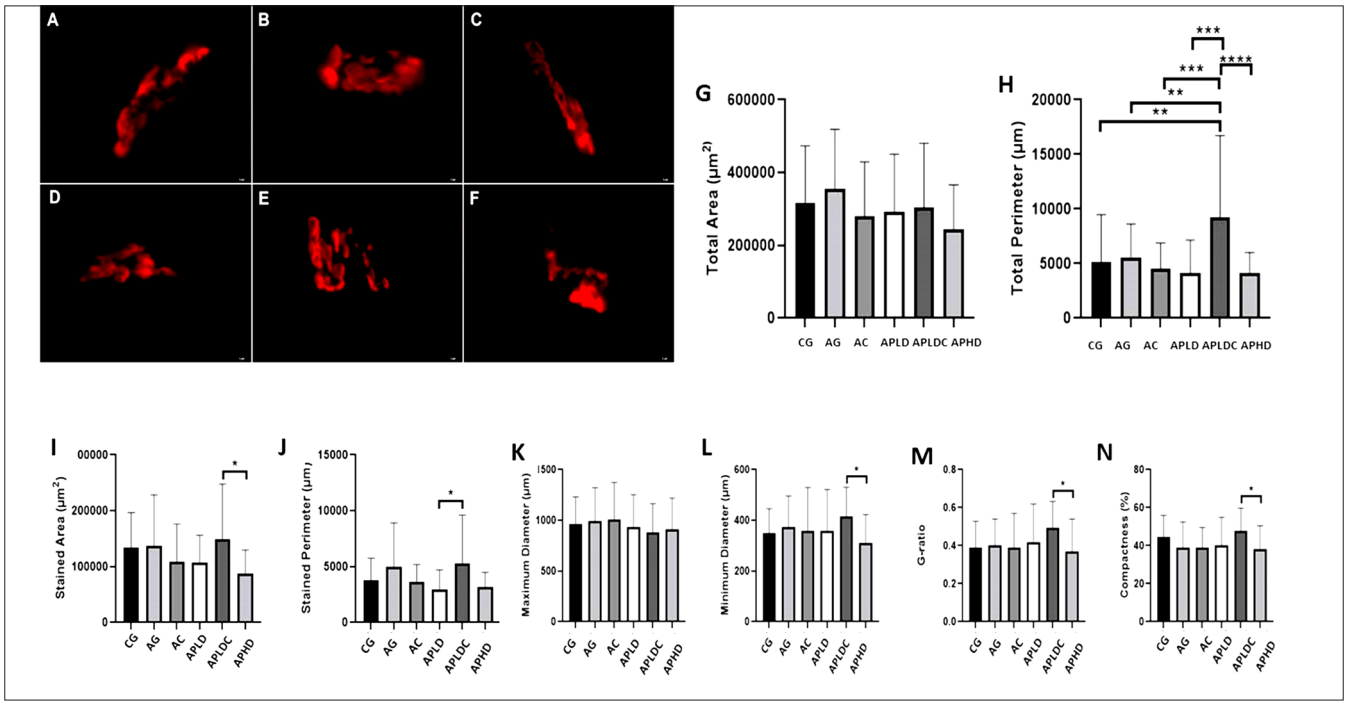


Figure 7. (A-F) Photomicrographs of neuromuscular junction postsynaptic region immunostaining of the experimental groups. The images show the different dispositions of the acetylcholine activation areas in relation to the protocols.

(A) Control Group (CG); **(B)** Arthritis Group (AG); **(C)** Arthritis Curcumin (AC); **(D)** Arthritis Prednisone Low-Dose (APLD); **(E)** Arthritis Prednisone High-Dose (APHD); **(F)** Arthritis Prednisone Low-Dose and Curcumin (APLDC); **(G-N)** Morphometrical analysis. A Kruskall-Wallis test Dun's post-test was used ($p = 0.05$); **(G)** Total Area; (**H)** Total Perimeter; (**I)** Stained Area; (**J)** Stained Perimeter; (**K)** Maximum Diameter; (**L)** Maximum Diameter; (**M)** Q-ratio; (**N)** Compactness.

important complication of RA, although experimental arthritis induces weight loss, there are evidences showing that wasting may happen partially due to the decrease in food intake (26).

APLDC had the best recovery when compared to all the others RA groups. There are evidences that curcumin's effects on metabolic disorders and autoimmune conditions may not only solely rely on its bioavailability and serum concentrations but also arise from its positive influence on gastrointestinal health and function (27).

Some studies demonstrated the effect of CM on weight gain (28), showed that oral administration of CM significantly increased body weight. In short, CM plays an important role in the metabolic and gastrointestinal system, through the maintenance of homeostasis.

Supplementation with curcumin improved functional aspects

Physical limitations afflicting RA patients were significantly associated with a reduced work productivity. A main cause to this limitation is muscle weakness, that refers to a decrease in muscle strength, what was also found in AG, in our work, and in RA patients it has often been attributed to a decrease in muscle mass due to myofibers atrophy (29).

Corroborating with our findings, Coradini *et al.* (2015) (30) showed that 1.75 mg/kg curcumin, significantly reduced the synovial membrane infiltration and fibrosis. The paw volume was also reduced after treatment with 100 mg/kg curcumin (16) and oral gavage treatment with CM have been reported as significantly decreased mechanical allodynia and heat hyperalgesia (31).

Functionality and the relationship with atrophy, degeneration of muscle spindles and increased collagen in the extracellular matrix in RA groups

Proprioception informs us about the contractile state and movement of muscles. Patients with RA have prominent sensory and motor deficits, generally leading to dysmetria with unsteady gait, variability in force and step length and reduced ability to identify the direction of joint movements (32).

In our study, RA groups presented decreased performance in the functional EVs and also degeneration in the muscle spindles. It is well known that the loss of proprio-

ceptive feedback may severely affect the motor function in mammals and is a symptom commonly associated with numerous neurological and orthopedic conditions (33).
We also found atrophy in the AR muscle fibers. Muscle spindle function has been related with muscular weakness and atrophy in combination with degeneration of the musculoskeletal system, leading to loss of contractile force and muscle failure (34).
AG also showed greater quantity of total collagen and type I. Excessive deposition of ECM results in muscle fibrosis, what impairs muscle function, affects muscle fiber regeneration after injury and increases muscle susceptibility to re-injury (35).

Greater perimeter in the postsynaptic region of APLDC

The muscular contraction is stimulated through motor neurons, connected to the activated muscle fibers through the NMJ. The acetylcholine released in the synaptic cleft interacts with specific receptors (AChR) and generates an action potential across the surface of the muscle cell, which diffuses rapidly within muscle tissue through a network of specialized tubules called T tubules (36). The action potential activates the dihydropyridine receptor opening allows the influx of calcium (Ca^{2+}) into the cytoplasm and stimulates the ryanodine receptors to release more Ca^{2+} from the sarcoplasmic reticulum, in turn, triggers the interaction between contractile proteins and causes shortening of muscle fiber (37).
The reduction in muscle functionality causes structural fragmentation and loss of NMJ function. Also, periods of physical inactivity or gravitational reduction affect the structure of NMJ, inducing changes in the pre and post synaptic components (38). NMJ has wide strands regarding its plasticity in the face of stimuli such as aging (sarcopenia), use of pharmacological drugs due to the direct relationship with the skeletal striated muscle, this correlation with the peripheral nervous system shows an adaptation of the muscle fibers to the pre- and post-synaptic activity of NMJ (39).
The present study demonstrated the postsynaptic region's morphological adaptations and changes in APLDC. Reduction in the postsynaptic cleft indicates the maintenance of the active zones that adapt and contribute with neurotransmission reducing the access distance from the synaptic vesicles to the Ca^{2+} channels (31). Contrary to that, increase in this region indicated that the association of the protocols promotes adaptations in old rats related to the NMJ density, decreasing with the arrival of aging and the protocol maintained their distribution as the main adaptation (40). The effects of muscle weakness and atrophy induced by joint immobilization cause similar effects on postsynaptic components according to the fiber innervation, decreasing its size (38). However, the effects of an intervention in the rehabilitation of skeletal muscle and the repercussions on NMJ neuroplasticity are not fully established.

PD treatment without supplementation did not have very promising results, in both low and high doses

In our study, the treatment with PD without CM supplementation had some positive results mainly in the functional EVs, but in histomorphometry, APLDC had better results. The glucocorticoids' use is frequently indicated in the treatment of rheumatoid diseases. However, the side-effects of glucocorticoids might include myopathy since it has a direct effect on increasing muscle protein degradation and inhibiting amino acid transport to muscle cells (41).
Besides that, glucocorticoids are reported as a powerful angiostatic and are used to treat angiogenesis-related diseases. Shikatani *et al.* (2012) (42), showed that corticosterone decreased the number of capillaries in rat skeletal muscle and inhibited proliferation, migration and sprouting of skeletal muscle microvascular endothelial cells *in vitro*.
Curiously, in our work, APHD had the opposite effect and presented de highest number of capillaries. Some studies have reported glucocorticoids administration can show divergent effects on altered blood flow. In growth restricted animal models, corticoids use alters cerebral blood flow, impairs brain growth, and was associated with brain damage (43).

AC did not have as promising results as APLDC

CM can attenuate RA by promoting the production of interleukin 10 (IL-10), which itself further reduces production of pro-inflammatory cytokines, and it can be used either single or in combination (44).
However, like PD, CM is hydrophobic, which limits their clinical application and their ability to target inflammation lesion. Studies have shown that this polyphenol has a poor pharmacokinetic profile. Moreover, CM pharmacological effects depend on intestinal interactions, possibly through an increase in somatostatin secretion (45).
Because of the low aqueous solubility, poor oral bioavailability and extensive hepatic metabolism, various formulations of curcumin, such as complexation, micelles, microemulsion, solid-lipid nanoparticles and solid dispersions have been developed to enhance efficacy and bioavailability (46).

PD treatment supplemented with CM had the most positive results

The combination of more than one type of drug component is often use in medicine. A particular strategy does not always enhance its specific pharmacological effect; combinations involving two or more components can provide additive and synergistic effects (47).

It has been reported that the use of CM associated with PD in CFA-induced RA model in rats reduces interleukin 1β and TNF α and increases IL-10 concentrations (48). Evaluated the clinical efficacy as a topical drug of a novel mixture of PD and CM in 60 patients of oral lichen planus and the mixture effectively reduced the reticulation, erosion and pain.

A study combining PD with CM provided the best therapeutic effect, suggesting that co-delivery of PD and CM could synergistically regulate the development of RA and potentially may be used as dual-agent therapy to treat RA (49).

In short, CM supplementation may represent a beneficial therapeutic agent for patients with RA and this co-delivering can act more specifically in inflamed tissues, thereby reducing the risk of adverse effects.

CONCLUSIONS

We concluded that RA can cause reduction in the functional parameters, degeneration in the rectus femoris muscular tissue and changes in postsynaptic morphometry. CM supplementation in the treatment with 2 mg/kg/day PD demonstrated the most positive effects in all analyzed parameters. In summary, a lower dose of PD may have more promising effects than the higher dose when used synergistically with the herbal supplement.

FUNDINGS

None.

DATA AVAILABILITY

Data are avilable under reasonable request to the corresponding author.

CONTRIBUTIONS

ACBR: conceptualization, data curation, analysis, investigation, methodology, project administration, supervision, visualization, writing – original draft. CDTB, DFSR: conceptualization, analysis, methodology, visualization. ACDS: conceptualization, investigation, methodology, visualization. JPN, APC: conceptualization, analysis, investigation, methodology, visualization, writing – original draft. MMT: conceptualization, methodology, supervision, writing – original draft. RMC: conceptualization, methodology, supervision, writing – review & editing. GRFB: conceptualization, data curation, formal analysis, investigation, methodology, project administration, software, supervision, visualization, writing – review & editing. LFCR, TS: conceptualization, data curation, formal analysis, investigation, methodology, project administration, supervision, validation, visualization, writing – review & editing.

CONFLICT OF INTERESTS

The authors declare that they have no conflict of interests.

ACKNOWLEDGEMENTS

We thank the State University of Western Paraná (UNIOESTE), São Paulo State University Júlio de Mesquita Filho (Unesp), the Coordination for the Improvement of Higher Education Personnel (CAPES), São Paulo Research Foundation (FAPESP), the Professor Doctor Katya Naliwaiko and technician Celeste da Rocha Paiva.

REFERENCES

1. Kumar P, Banik S. Pharmacotherapy options in rheumatoid arthritis. Clin Med Insights Arthritis Musculoskelet Disord. 2013;6:35-43. doi: 10.4137/CMAMD.S5558.
2. Smolen JS, Landewé RBM, Bijlsma JWJ, et al. EULAR recommendations for the management of rheumatoid arthritis with synthetic and biological disease-modifying antirheumatic drugs: 2019 update. Ann Rheum Dis. 2020;79(6):685-99. doi: 10.1136/annrheumdis-2019-216655.
3. Lu W, Zhou Z, Naqvi SMAS, et al. Meta-analysis on efficacy and safety of modified guizhi shaoyao zhimu tang with the western medicines in treating rheumatoid arthritis. Yangtze Med. 2018;2:161-70. doi: 10.4236/ym.2018.23017.
4. Kamada Y, Toyama S, Arai Y, et al. Treadmill running prevents atrophy differently in fast- versus slow-twitch muscles in a rat model of rheumatoid arthritis. J Muscle Res Cell Motil. 2021;42(3-4):429-41. doi: 10.1007/s10974-021-09610-0.
5. Oishi S, Wendling D, Sibilia J, et al. Treatment of active rheumatoid arthritis: comparison of patients younger vs older than 75 years (CORPUS cohort). Hum Vaccin Immunother. 2018;14(11):2612-7. doi: 10.1080/21645515.2018.1522470.

6. Li C, Li H, Wang Q, et al. pH-sensitive polymeric micelles for targeted delivery to inflamed joints. J Control Release. 2017;28(246):133-41. doi: 10.1016/j.jconrel.2016.12.027.
7. Zhou M, Hou J, Zhong Z, et al. Targeted delivery of hyaluronic acid-coated solid lipid nanoparticles for rheumatoid arthritis therapy. Drug Deliv. 2018;25(1):716-22. doi: 10.1080/10717544.2018.1447050.
8. Smolen JS, Aletaha D, McInnes IB. Rheumatoid arthritis. Lancet. 2016;388(10055):2023-38. doi: 10.1016/S0140-6736(16)30173-8.
9. Lemmey AB, Wilkinson TJ, Clayton RJ, et al. Tight control of disease activity fails to improve body composition or physical function in rheumatoid arthritis patients. Rheumatology (Oxford). 2016;55(10):1736-45. doi: 10.1093/rheumatology/kew243.
10. Li XZ, Zhang SN. Herbal compounds for rheumatoid arthritis: Literatures review and cheminformatics prediction. Phytother Res. 2020;34(1):51-66. doi: 10.1002/ptr.6509.
11. Asteriou E, Gkoutzourelas A, Mavropoulos A, et al. Curcumin for the Management of Periodontitis and Early ACPA-Positive Rheumatoid Arthritis: Killing Two Birds with One Stone. Nutrients. 2018;10(7):908. doi: 10.3390/nu10070908.
12. Bagherniya M, Darand M, Askari G, et al. The Clinical Use of Curcumin for the Treatment of Rheumatoid Arthritis: A Systematic Review of Clinical Trials. Adv Exp Med Biol. 2021;(1291):251-63. doi: 10.1007/978-3-030-56153-6_15.
13. Dei Cas M, Ghidoni R. Dietary Curcumin: Correlation between Bioavailability and Health Potential. Nutrients. 2019;11(9):2147. doi: 10.3390/nu11092147.
14. Zimmermann M. Ethical guidelines for investigations of experimental pain in conscious animals. Pain. 1983;16(2):109-10. doi: 10.1016/0304-3959(83)90201-4.
15. de Freitas Tavares AL, Neves M, Schnaufer TC, et al. Therapeutic Effect of Aquatic Resistance Exercise on Rectus Femoris and Knee in a Model of Rheumatoid Arthritis. Muscles Ligaments Tendons J. 2022;12(3):267-78. doi: 10.32098/mltj.03.2022.02.
16. Nonose N, Pereira JA, Machado PR, et al. Oral administration of curcumin (Curcuma longa) can attenuate the neutrophil inflammatory response in zymosan-induced arthritis in rats. Acta Cir Bras. 2014;29(11):727-34. doi: 10.1590/s0102-86502014001800006.
17. Masibo KM, Mwonjoria J, Mburu D. Efficacy and Safety of Prednisolone in the Management of Alcohol-Induced Adverse Effects in a Rat Model. J Alcohol Drug Depend. 2020;5:(8):1-8. doi: 10.35248/2329-6488.20.8.334.
18. Zhang Z, Chen L, Ni H. The effectiveness of Corticosteroids on mortality in patients with acute respiratory distress syndrome or acute lung injury: a secondary analysis. Sci Rep. 2015;2(5):17654. doi: 10.1038/srep17654.
19. Tilson HA, Cabe PA. The effects of acrylamide given acutely or in repeated doses on fore- and hindlimb function of rats. Toxicol Appl Pharmacol. 1979;47(2):253-60. doi: 10.1016/0041-008x(79)90319-3.
20. Bertelli JA, Mira JC. The grasping test: a simple behavioral method for objective quantitative assessment of peripheral nerve regeneration in the rat. J Neurosci Methods. 1995;58(1-2):151-5. doi: 10.1016/0165-0270(94)00169-h.
21. Yonemori F, Yamaguchi T, Yamada H, et al. Evaluation of a motor deficit after chronic focal cerebral ischemia in rats. J Cereb Blood Flow Metab. 1998;18(10):1099-106. doi: 10.1097/00004647-199810000-00006.
22. Chaplan SR, Bach FW, Pogrel JW, et al. Quantitative assessment of tactile allodynia in the rat paw. J Neurosci Methods. 1994;53(1):55-63. doi: 10.1016/0165-0270(94)90144-9.
23. DeGirolami UU, Smith TW. Teaching monograph: pathology of skeletal muscle diseases. Am J Pathol. 1982;107(2):231-76.
24. Zazula MF, de Andrade BZ, Toni Boaro C, et al. Development of a histopathological index for skeletal muscle analysis in Rattus norvegicus (Rodentia: Muridae). Acta Histochem. 2022;124(4):151892. doi: 10.1016/j.acthis.2022.151892.
25. Zazula MF, Marca AP, Oliveira MC, et al. Peripubertal Exposure to Glyphosate-Based Herbicides Promotes Histopathological Impairment in the Structure of the Diaphragm Muscle of C57BL/6 Mice. Muscles Ligaments Tendons J. 2024;14 (1):12-21 doi: 10.32098/mltj.01.2024.02.
26. Castillero E, Martín AI, López-Menduiña M, et al. IGF-I system, atrogenes and myogenic regulatory factors in arthritis induced muscle wasting. Mol Cell Endocrinol. 2009;309(1-2):8-16. doi: 10.1016/j.mce.2009.05.017.
27. Lopresti AL. The Problem of Curcumin and Its Bioavailability: Could Its Gastrointestinal Influence Contribute to Its Overall Health-Enhancing Effects? Adv Nutr. 2018;9(1):41-50. doi: 10.1093/advances/nmx011.
28. Alghadir A, Miraj M, Ali S. Efficacy of Curcumin with Iontophoretic Application on Paw Edema and Hematological Responses in Collagen-Induced Arthritis Rat Models. Evid Based Complement Alternat Med. 2020;(9):4606520. doi: 10.1155/2020/4606520.
29. Londhe P, Guttridge DC. Inflammation induced loss of skeletal muscle. Bone. 2015;(80):131-42. doi: 10.1016/j.bone.2015.03.015.
30. Coradini K, Friedrich RB, Fonseca FN, et al. A novel approach to arthritis treatment based on resveratrol and curcumin co-encapsulated in lipid-core nanocapsules: In vivo studies. Eur J Pharm Sci. 2015;(78):163-70. doi: 10.1016/j.ejps.2015.07.012.
31. Chen JJ, Dai L, Zhao LX, et al. Intrathecal curcumin attenuates pain hypersensitivity and decreases spinal neuroinflammation in rat model of monoarthritis. Sci Rep. 2015;19(5):10278. doi: 10.1038/srep10278.
32. Masingue M, Faure J, Sole G, Stojkovic T, Leonard-Louis S. A novel nonsense PIEZO2 mutation in a family with scoliosis and proprioceptive defect. Neuromusc Disord. 2019;29:75-9. doi: 10.1016/j.nmd.2018.10.005.
33. Mayer WP, Akay T. Stumbling corrective reaction elicited by mechanical and electrical stimulation of the saphenous nerve in walking mice. J Exp Biol. 2018;(10):221(Pt 13):jeb178095. doi: 10.1242/jeb.178095.
34. Mosqueira M, Zeiger U, Förderer M, et al. Cardiac and respiratory dysfunction in Duchenne muscular dystrophy and the role of second messengers. Med Res Rev. 2013;33(5):1174-213. doi: 10.1002/med.21279.
35. Prazeres PHDM, Turquetti AOM, Azevedo PO, et al. Perivascular cell αv integrins as a target to treat skeletal muscle fibrosis. Int J Biochem Cell Biol. 2018;(99):109-13. doi: 10.1016/j.biocel.2018.04.002.

36. Lovering RM, Iyer SR, Edwards B, et al. Alterations of neuromuscular junctions in Duchenne muscular dystrophy. Neurosci Lett. 2020;(737):135304. doi: 10.1016/j.neulet.2020.135304.
37. Gonzalez-Freire M, Semba RD, Ubaida-Mohien C, et al. The Human Skeletal Muscle Proteome Project: a reappraisal of the current literature. J Cachexia Sarcopenia Muscle. 2017;8(1):5-18. doi: 10.1002/jcsm.12121.
38. Deschenes MR, Tenny KA, Wilson MH. Increased and decreased activity elicits specific morphological adaptations of the neuromuscular junction. Neuroscience. 2006;137(4):1277-83. doi: 10.1016/j.neuroscience.2005.10.042.
39. Deschenes MR, Tufts HL, Oh J, et al. Effects of exercise training on neuromuscular junctions and their active zones in young and aged muscles. Neurobiol Aging. 2020;(95):1-8. doi: 10.1016/j.neurobiolaging.2020.07.001.
40. Tintignac LA, Brenner HR, Rüegg MA. Mechanisms Regulating Neuromuscular Junction Development and Function and Causes of Muscle Wasting. Physiol Rev. 2015;95(3):809-52. doi: 10.1152/physrev.00033.2014.
41. Zhao D, Zhang F, Wang B, et al. Guidelines for clinical diagnosis and treatment of osteonecrosis of the femoral head in adults (2019 version). J Orthop Translat. 2020;(21):100-10. doi: 10.1016/j.jot.2019.12.004.
42. Shikatani EA, Trifonova A, Mandel ER, et al. Inhibition of proliferation, migration and proteolysis contribute to corticosterone-mediated inhibition of angiogenesis. PLoS One. 2012;7(10):e46625. doi: 10.1371/journal.pone.0046625.
43. Kaiser JR, Bai S, Gibson N, et al. Association Between Transient Newborn Hypoglycemia and Fourth-Grade Achievement Test Proficiency: A Population-Based Study. JAMA Pediatr. 2015;169(10):913-21. doi: 10.1001/jamapediatrics.2015.1631.
44. Anthwal A, Thakur BK, Rawat MS, et al. Synthesis, characterization and in vitro anticancer activity of C-5 curcumin analogues with potential to inhibit TNF-α-induced NF-κB activation. Biomed Res Int. 2014;2014:524161. doi: 10.1155/2014/524161.
45. Cheng D, Li W, Wang L, et al. Pharmacokinetics, Pharmacodynamics, and PKPD Modeling of Curcumin in Regulating Antioxidant and Epigenetic Gene Expression in Healthy Human Volunteers. Mol Pharm. 2019;16(5):1881-9. doi: 10.1021/acs.molpharmaceut.8b01246.
46. Stohs SJ, Chen O, Ray SD, et al. Highly Bioavailable Forms of Curcumin and Promising Avenues for Curcumin-Based Research and Application: A Review. Molecules. 2020;25(6):1397. doi: 10.3390/molecules25061397.
47. Chou TC. Theoretical basis, experimental design, and computerized simulation of synergism and antagonism in drug combination studies. Pharmacol Rev. 2006;58(3):621-81. doi: 10.1124/pr.58.3.10.
48. Naik SR, Gupta P, Ashok L, et al. A novel mixture of curcumin paste and prednisolone for treating oral lichen planus: A case controlled comparative study. J. Indian Acad. Oral Med. Radiol. 2019;(31):286-92. doi: 10.4103/jiaomr.jiaomr_171_19.
49. Hayakawa T, Yaguchi T, Kawakami Y. Enhanced anti-tumor effects of the PD-1 blockade combined with a highly absorptive form of curcumin targeting STAT3. Cancer Sci. 2020;111(12):4326-35. doi: 10.1111/cas.14675.